Observation and modeling of the suction pump effect during rapid dilatant slip

Observation and modeling of the suction pump effect during rapid dilatant slip

Eric Grueschow
Department of Mechanical Engineering, Northwestern University, Evanston, Illinois, USA

Ohmyoung Kwon[1] and Ian G. Main
School of Geosciences, University of Edinburgh, Edinburgh, UK

John W. Rudnicki
Department of Civil and Environmental Engineering, Northwestern University, Evanston, Illinois, USA

Received 18 July 2002; revised 18 July 2002; accepted 22 January 2003; published 11 March 2003.

[1] The temporary pressure drop observed during post-peak dilatant slip in axi-symmetric testing of a porous aeolian sandstone is modeled using a simple function of opening caused by sliding along the fault surface. Results suggest dilatancy of 0.02 mm accompanying frictional sliding, less than 10% of the typical grain diameter of 0.25–0.50 mm. The rapid void opening, under nominally undrained conditions at constant upstream flow rate, causes a strong 'suction pump' effect. A theoretical maximum pressure drop of 0.09 MPa or more, consistent with the experimentally measured results, can occur without a change in permeability properties. *INDEX TERMS:* 5114 Physical Properties of Rocks: Permeability and porosity; 5104 Physical Properties of Rocks: Fracture and flow; 5199 Physical Properties of Rocks: General or miscellaneous. **Citation:** Grueschow, E., O. Kwon, I. G. Main, and J. W. Rudnicki, Observation and modeling of the suction pump effect during rapid dilatant slip, *Geophys. Res. Lett.*, *30*(5), 1226, doi:10.1029/2002GL015905, 2003.

1. Introduction

[2] Dilatancy during frictional sliding in laboratory samples has been observed by several workers [*Barton*, 1976; *Jamison and Teufel*, 1979; *Teufel*, 1981]. During dilatant slip, the observed shear stress decreased from a peak value to a nearly constant residual value [*Barton*, 1972, 1973]. Similar results were obtained for frictional slip in axi-symmetric compression experiments [*Rice*, 1977, 1980; *Wong*, 1982], requiring evaluation of normal stress effects. *Zoback and Byerlee* [1975] and *Brace et al.* [1968] were able to show that cracking prior to peak stress greatly increased permeability in some cases. *Olsson and Brown* [1993] were able to relate permeability changes to fracture surface topography.

[3] Most of these studies were based on the properties of crystalline rocks, although pre-and post-peak dilatancy is also seen in sedimentary rocks, usually after an initial compaction phase. For example *Mair et al.* [2000] showed dilatancy during the sequential growth of deformation bands in a porous aeolian sandstone (Locharbriggs) deformed under dry conditions. Her microstructural observations were used to predict the evolution of the permeability as a function of strain and porosity in Clashach sandstone during the quasi-static phases of deformation [*Main et al.*, 2000]. However, this model fails to account for the significant drop in upstream fluid pressure observed during the strain softening period after peak stress and at the onset of dynamic faulting. One possible explanation for the pressure drop is a rapid increase in permeability due to the formation of new microcracks. Alternatively, this transient pressure drop represented by the apparent permeability spike may be due to a 'suction pump' effect in a saturated medium, where rapid dilatant slip on the fault plane under nominally undrained conditions leads to a lower upstream pressure required to maintain the same servo-controlled flow rate [*Main et al.*, 2001]. Here we use *Rudnicki and Chen*'s [1988] model of coupled frictional slip and fluid flow to demonstrate that the observed upstream pressure drop can be adequately explained by rapid dilatant slip, without necessarily invoking change in material properties such as cross-fault permeability.

2. Experimental Setup

[4] The experimental set-up is described in *Mair et al.* [2000] and *Main et al.* [2000]. A large-capacity (2MN) deformation rig was used to deform right cylindrical samples of 100 mm diameter by 200–250 mm length, with confining pressures up to 70 MPa. Core samples were obtained from the Clashach quarry (Hopeman sandstone) near Lossiemouth, Scotland. This Permian sandstone is a medium-to-coarse grained (0.25–0.50 mm diameter) sub-arkosic arenite, consisting of sub-rounded quartz grains (90%) and K-feldspar (10%) and a minor fraction of detrital minerals, with a starting porosity of ~20%. Samples were initially saturated with either oil or water, which then formed an appropriate permeant for the permeability measurements. In the test used to validate the model here, oil was used as the permeant. Permeability was determined from the difference of fluid pressures across the sample (dP) to deliver constant flow rate of 2cc/min to the upstream reservoir. The fluid pressure of the downstream reservoir was maintained constant at 6.9 MPa by using a back-pressure regulator. The sample was strained at a rate of 5×10^{-6} s^{-1}, while maintaining a constant confining

[1]Now at Core Laboratories, Houston, Texas, USA.

0094-8276/03/2002GL015905

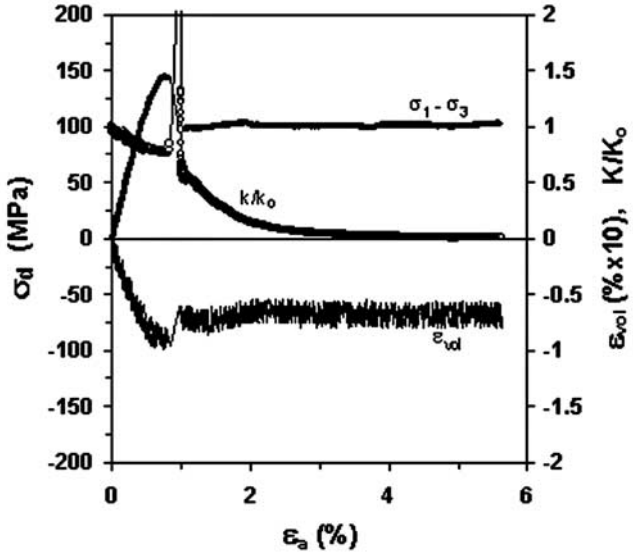

Figure 1. Differential stress (σ_d), volumetric strain (ε_{vol}), normalized permeability (K/K_o) as a function of axial strain (ε_a) for the Hopeman sandstone sample used for the rapid dilatant slip model. Notice that the scale for the volumetric strain is vertically exaggerated by a factor of 10 to plot in the same figure as the normalized permeability (Y-2 axis).

pressure of 41.4 MPa at room temperature. The volumetric strain is measured from the change in confining fluid volume required to maintain constant confining pressure by servo-control. Permeability data were logged in at three-second intervals.

[5] Figure 1 shows the differential stress σ_d, volumetric strain ε_{vol}, and permeability as a function of axial strain ε_a for the Hopeman sandstone sample used in this study. The inferred permeability K was normalized by the initial permeability K_o of 4.8×10^{-13} m^2. The sample compacts initially and the permeability decreases upon increasing differential stress. At the time of failure, increase in the volumetric strain was observed with accompanying transient pressure drop. This transient pressure drop is represented by the transient apparent permeability increase at the time of failure in Figure 1. After the transient increase, the permeability continuously decreases with increasing axial strain during post-failure sliding period.

3. Theoretical Framework

3.1. Modeling of Strain and Opening

[6] The model of frictional slip used by *Rudnicki and Chen* [1988] (hereinafter referred to as RC) can be used for the fractured specimen. In RC, the sample is modeled as an elastic body sliding along a fracture surface. As can be seen in Figure 2, by arranging the fracture surface at an angle, θ, and treating the top and bottom portions as separate bodies, they were able to simulate post-peak sliding during axi-symmetric testing. During sliding, the void space increases by a distance 2Δ. The total relative slip between the surfaces during sliding is 2δ, and the measured displacement of the sample end is u_{ax}.

[7] The observed volume strain and axial strain are used to estimate the sliding and opening values. The volumetric strain is measured from the change in confining fluid volume by servo control. The servo-control system adds a significant amount of noise to this measurement, too much to yield a good estimate for the evolution of void opening with slip. Because of this, the measured volumetric strain was only used to estimate the maximum opening, Δ_o, as a function of the sliding length corresponding with maximum opening, δ_o. Estimates for δ_o were made in order to fit the data.

[8] The cause of the measured volume strain is void opening. The volume of an opening along an oblique fault can be estimated as $2\Delta\pi R^2/cos\theta$, where R is the specimen radius and θ is the angle of the fault surface. Pure sliding along the fault causes no additional change in volume strain. With elastic relations, opening volume, and the volume strain definition, it is determined that

$$\varepsilon_{vol} = \frac{2\Delta}{L\cos\theta} + \frac{(\sigma_d - \sigma_d^p)(1-2\nu)}{E}, \qquad (1)$$

where σ_d is the stress difference, σ_d^p is the value of stress difference at peak stress, L is the specimen length, and E and ν are elastic properties of the material. The volume strain, ε_{vol}, is zeroed at peak stress. The first term results from the void volume change due to dilation of the fault. The second term is the volumetric elastic response for constant confining stress. Comparison of (1) to the data for stress and volumetric strain yields an estimate for Δ_o of 0.02 mm, i.e. less than 10% of the typical grain diameter of 0.25–0.50 mm. This implies that grains are not simply riding intact over each other, but some shearing off and grain fracture is reducing the magnitude of the opening dilatancy, consistent with the observation of comminuted fault gouge after the test.

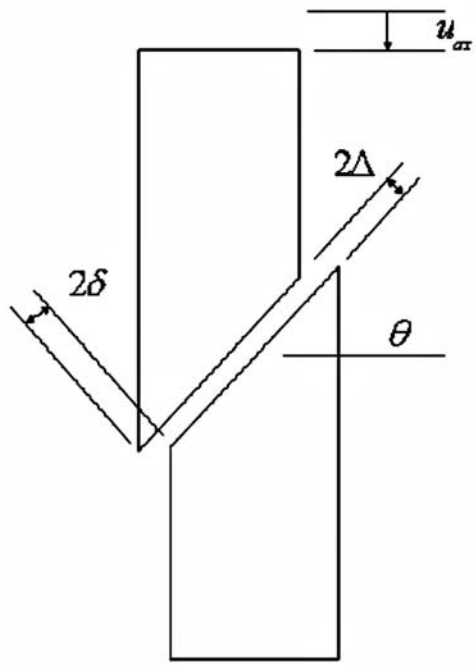

Figure 2. Geometry of the problem. Two slabs are loaded in axi-symmetric compression, separated by a fault zone at angle θ. The relative slip between the slabs is 2δ, and the dilatant opening between the surfaces is 2Δ. The measured displacement of the end of the specimen is u_{ax}.

[9] The relation between δ and Δ given in RC,

$$\Delta = \Delta_o\left[2(\delta/\delta_o) - (\delta/\delta_o)^2\right], \tag{2}$$

was used to estimate Δ. After δ reaches δ_o, the opening remains constant. This relation is a simple function meeting reasonable assumptions about opening behavior, and is not meant as a fundamental law. The best fit for the length δ_o was 0.6 mm. This estimate seems reasonable [*Dieterich*, 1978, 1979; *Rice*, 1980; *Wong*, 1982].

[10] RC also gives the axial strain in terms of both δ and Δ. Some rearranging and substitutions yield

$$\varepsilon_{ax} = \frac{2(\delta\sin\theta - \Delta\cos\theta)}{L} + \frac{(\sigma_d - \sigma_d^p)}{E}. \tag{3}$$

[11] Combining (2) and (3) and rearranging yields

$$\varepsilon_{ax} - \frac{(\sigma_d - \sigma_d^p)}{E} = \frac{2}{L}\left\{\delta\sin\theta - \Delta_o\cos\theta\left[2\left(\frac{\delta}{\delta_o}\right) - \left(\frac{\delta}{\delta_o}\right)^2\right]\right\}. \tag{4}$$

This equation can be used to solve for sliding and opening after peak stress. The bracketed term on the right reaches unity when $\delta \geq \delta_o$.

3.2. Modeling of Fluid Flow

[12] The geometry for the model of fluid flow throughout the specimen is shown in Figure 3. The model boundary conditions are the same for the experimental test, with downstream pressure and upstream flow rate held constant, and the upstream pressure allowed to vary. The length of each body, h_p, is assumed to be half the specimen length.

[13] The predicted pressure drop is determined using the opening estimate and measured stress and strain data. Because the dilatant slip is so rapid, information between data points is interpolated, assuming constant strain rate.

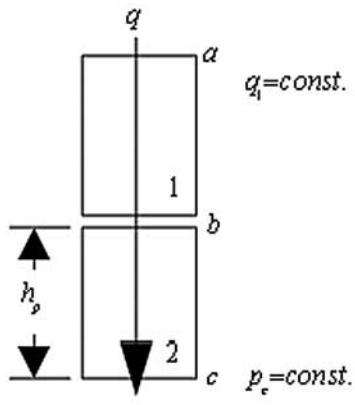

Figure 3. Schematic diagram of the flow model. The angle θ is ignored for simplicity. The top and bottom slabs are labeled 1 and 2. The pressure is held constant at point *c*, and measured at point *a*. The flow rate *q* into the specimen is held constant. The fault surface is signified by point *b*. Each body has a length h_p.

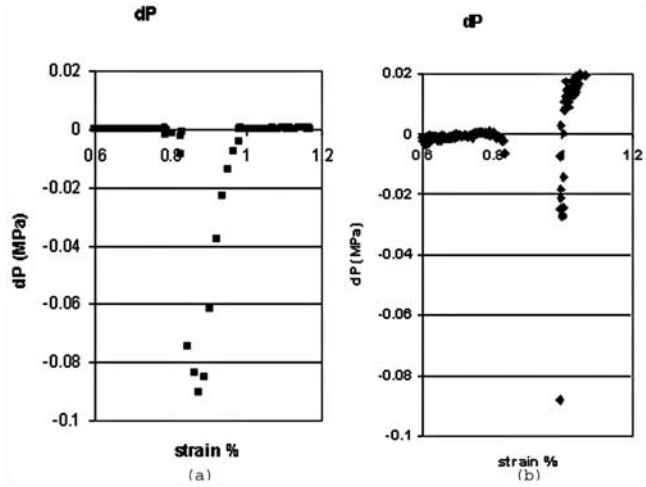

Figure 4. Pressure change due to dilatant slip. (a) Modeled pressure change assuming no change in permeability and constant strain rate between data points. (b) Observed pressure change. The sampling rate in the experiment was too slow to resolve the details of the pressure spike.

[14] A linear pressure gradient is assumed for the fluid flow through each segment of the specimen. This assumption is the same as that made by RC, and is consistent with Darcy's Law for steady state flow. Since the flow rate into the specimen is constant,

$$dq_1 = 0 = \frac{\rho K}{h_p}(dp_a - dp_b), \tag{5}$$

where q is the flow rate per area, K is the permeability, ρ is the density, and p is the pressure at the given point within the model. The prefix d is used to signify an incremental change in the pressure, rather than a time derivative.

[15] As the fault opened, the flow out of the specimen was reduced. The reduction can be modeled as

$$\frac{d}{dt}(2\rho\Delta) = q_1 - q_2 = \frac{\rho K}{h_p}(dp_b). \tag{6}$$

If the density and permeability are assumed constant, combining (2), (5) and (6) gives

$$dp_a = \frac{2\Delta_o L}{\delta_o K}(1 - \delta/\delta_o)\dot{\delta}, \tag{7}$$

where L is the total length of the specimen.

[16] Equations (4) and (7) can be combined to determine the dp_a for the discrete data points. The dilatant slip is too rapid, however, to adequately evaluate the pressure spike with these data alone. Strain was linearly interpolated between the existing data points, corresponding to three seconds of dilatant slip. Stress interpolation was fit to the RC relation

$$\tau = \tau_p - (\tau_p - \tau_r)\left[-2(\delta/\delta_o)^3 + 3(\delta/\delta_o)^2\right], \tag{8}$$

where τ is shear stress and subscripts p and r refer to the peak and residual values.

[17] Figure 4 shows the theoretical and observed results. The plot on the left is the calculated pressure spike due to

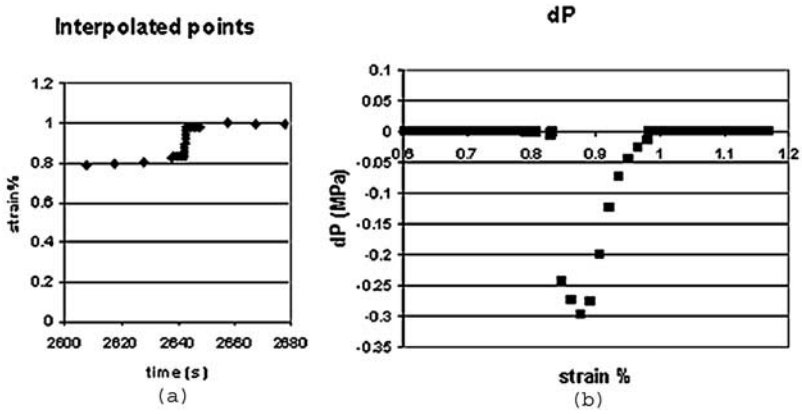

Figure 5. Pressure change due to dilatant slip with an increased strain rate. (a) Assumed strain response between data points. Introductory and final strain rates are assumed the same as before faulting. Increased strain rate due to faulting is assumed to occur within one second. (b) Modeled pressure change without change in permeability properties with the strain behavior in (a). A significant increase in pressure change accompanies the change in strain rate.

(7), with a peak of magnitude 0.09 MPa. The plot on the right shows the measured pressure spike. The sampling rate was too slow to resolve the details of the pressure drop, but the lowest registered data point has a magnitude of 0.09 MPa.

[18] The strain rate increased substantially during dilatant slip. Consequently, the constant strain rate assumption used during interpolation is likely to significantly underestimate the rate of dilatant slip and the magnitude of the pressure spike. With interpolation assuming the constant increased strain rate to occur entirely within one second and the strain rate for the rest of the interpolation matching that for before and after faulting, as shown in Figure 5, a spike with a magnitude of 0.3 MPa occurs. Further increases in slip rate further increase the spike magnitude. Further resolution of this effect will require faster sampling rates in future experiments.

4. Conclusions

[19] We have used the coupled deformation-fluid flow model of *Rudnicki and Chen* [1988] to test the hypothesis that an observed upstream pressure drop during dynamic dilatant slip can be explained solely by the suction pump effect at constant flow rate. The result is positive, and quantitatively confirms the strength of the effect for rapid dilatant slip. No absolute change in bulk sample permeability is required to explain the laboratory observations. The inferred maximum dilatancy is 0.02 mm, i.e. less than 10% of the initial grain size. This implies that grains are not simply riding intact over each other, but some shearing off and grain fracture is reducing the magnitude of the opening dilatancy, consistent with the observation of comminuted fault gouge after the test.

[20] **Acknowledgments.** The experimental programme was funded jointly by BP, Exxon-Mobil, the Japanese National Oil Corporation, LASMO, Shell and Statoil. Partial financial support for work at Northwestern University was provided by U.S. Dept. of Energy, Basic Energy Sciences Grant No. DE-FG02-93ER14344.

References

Barton, N., A model study of rock joint deformation, *Int. J. Mech. Min. Sci.*, *9*, 579–602, 1972.

Barton, N., Review of the new shear strength criterion for rock joints, *Eng. Geol. Amsterdam*, *7*, 287–332, 1973.

Barton, N., The shear strength of rock and rock joints, *Int. J. Mech. Min. Sci. Geomech. Abstr.*, *13*, 255–279, 1976.

Brace, W. F., J. B. Walsh, and W. T. Frangos, Permeability of granite under high pressure, *J. Geophys. Res.*, *73*, 2225–2236, 1968.

Dieterich, J. H., Time-dependent friction and the mechanics of stick-slip, *Pure Appl. Geophys.*, *116*, 790–806, 1978.

Dieterich, J. H., Modeling of rock friction, 1, Experimental results and constitutive equations, *J. Geophys. Res.*, *84*, 2161–2168, 1979.

Jamison, W. R., and L. W. Teufel, Pore volume changes associated with failure and frictional sliding of a porous sandstone, in *Proceedings of the 20th U.S. Symposium on Rock Mechanics*, pp. 163–170, 1979.

Main, I. G., O. Kwon, B. T. Ngwenya, and S. C. Elphick, Fault sealing during deformation band growth in porous sandstone, *Geology*, *28*, 1131–1134, 2000.

Main, I., K. Mair, O. Kwon, S. Elphick, and B. Ngwenya, Experimental constraints on the mechanical and hydraulic properties of deformation bands in porous sandstones: A review, in *The Nature and Significance of Fault Zone Weakening*, edited by R. E. Holdsworth et al., *Geol. Soc. Spec. Publ.*, *186*, 43–63, 2001.

Mair, K., I. G. Main, and S. C. Elphick, Sequential development of deformation bands in the laboratory, *J. Struct. Geol.*, *22*, 25–42, 2000.

Olsson, W. A., and S. R. Brown, Hydromechanical response of a fracture undergoing compression and shear, *Int. J. Mech. Min. Sci.*, *30*, 845–851, 1993.

Rice, J. R., Pore pressure effects in inelastic constitutive formulations for fissured rock masses, in *Advances in Civil Engineering Through Engineering Mechanics: Proceedings, Second Annual Engineering Mechanics Division Specialty Conference, North Carolina State University, Raleigh, North Carolina, USA, May 23–25, 1977*, pp. 360–363, Am. Soc. Civ. Eng., New York, 1977.

Rice, J. R., The mechanics of earthquake rupture, in *Physics of the Earth*'s *Interior*, edited by A. M. Dziewonski and E. Boschi, *Proc. Int. Sch. Phys. Enrico Fermi*, *78*, 555–649, 1980.

Rudnicki, J. W., and C.-H. Chen, Stabilization of rapid frictional slip on a weakening fault by dilatant hardening, *J. Geophys. Res.*, *93*, 4745–4757, 1988.

Teufel, L. W., Pore volume changes during frictional sliding of simulated faults, in *Mechanical Behavior of Crustal Rocks*, *Geophys. Monogr. Ser.*, vol. 24, edited by N. L. Carter et al., pp. 135–145, AGU, Washington D. C., 1981.

Wong, T.-F., Shear fracture energy of Westerly granite from post-failure behavior, *J. Geophys. Res.*, *87*, 990–1000, 1982.

Zoback, M. D., and J. D. Byerlee, The effect of microcrack dilatancy on the permeability of Westerly granite, *J. Geophys. Res.*, *80*, 752–755, 1975.

O. Kwon, Core Laboratories, 6316 Windfern Road, Houston, TX 77040, USA. (okwon@corelab.com)

E. Grueschow and J. W. Rudnicki, Department of Mechanical Engineering, Northwestern University, 2145 Sheridan Road, Evanston, IL 60208, USA. (e-grueschow@northwestern.edu; jwrudn@northwestern.edu)

I. Main, School of Geosciences, University of Edinburgh, West Mains Road, Edinburgh EH9 3JW, UK. (ian.main@ed.ac.uk)